

Theoretical study of anisotropy spin-orbit coupling and local lattice structure for Fe^{3+} ions in $\text{MgTiO}_3:\text{Fe}^{3+}$ system*

H. Wang¹, X.-Y. Kuang^{1,2,a}, X.-F. Huang¹, D. Die³, and X. Yang¹

¹ Institute of Atomic and Molecular Physics, Department of physics, Sichuan University, Chengdu 610065, China

² International Centre for Materials Physics, Academia Sinica, Shengyang 110016, China

³ Institute of Applied Physics, Xihua University, Chengdu 610039, China

Received 29 June 2005 / Received in final form 28 November 2005

Published online 19 January 2006 – © EDP Sciences, Società Italiana di Fisica, Springer-Verlag 2006

Abstract. The anisotropy spin-orbit coupling matrices for a d^5 configuration ion in a trigonal ligand-field have been established. On basis of the anisotropy spin-orbit coupling matrices, the ground state zero-field splitting of the Fe^{3+} ions in ilmenite-structure $\text{MgTiO}_3:\text{Fe}^{3+}$ system has been studied. The calculated results show that the anisotropy of Fe^{3+} ions in the diamagnetic ilmenite MgTiO_3 is important and the EPR parameters depend sensitively on the anisotropy divergent parameter. Moreover, the effect of the anisotropy divergent parameter on the second-order parameter D is obviously larger than that on the fourth-order parameter $(a - F)$. Based on this point, the local lattice structure of Fe^{3+} ion in $\text{MgTiO}_3:\text{Fe}^{3+}$ system is determined by diagonalizing the complete energy matrices for a d^5 configuration ion in a trigonal ligand-field and considering the second-order as well as the fourth-order EPR parameters D and $(a - F)$ simultaneously. Our results are consistent with the experimental proposal that Fe^{3+} ions may locate at both the Mg^{2+} and Ti^{4+} sites.

PACS. 71.70.Gm Exchange interactions – 75.30.Et Exchange and superexchange interactions – 71.70.Ch Crystal and ligand fields

1 Introduction

MgTiO_3 is a diamagnetic oxide which has the trigonal crystal structure of ilmenite (FeTiO_3). The structure of MgTiO_3 is similar to that of Al_2O_3 , both the Mg^{2+} and Ti^{4+} cations occupy octahedrally-coordinated lattice with C_3 symmetry [1–8]. In the present paper, we will report the results of a general survey of the anisotropy of Fe^{3+} ion in $\text{MgTiO}_3:\text{Fe}^{3+}$ system, the effects of the anisotropy on the ground state zero-field splitting, as well as the EPR calculation for Fe^{3+} ion in MgTiO_3 crystal. The initial motivation for this study is that although some researches have studied the ground state zero-field splitting of $\text{MgTiO}_3:\text{Fe}^{3+}$ system theoretically, most of these theoretical researches only focused on the low-symmetry second-order parameter D [6,7]. Since both the EPR parameters D and $(a - F)$ relate to the trigonal ligand-field, herein, we suggest that the two low-symmetry parameters D and $(a - F)$ should be simultaneously considered in the description of the 6A_1 ground state splitting. In the investigation of the $\text{MgTiO}_3:\text{Fe}^{3+}$ system, we note that the low-symmetry EPR parameters D and $(a - F)$ cannot be reasonably explained simultaneously until the anisotropy

of Fe^{3+} ion in antiferromagnetic ilmenite MgTiO_3 is considered. Our study of ground state zero-field splitting for Fe^{3+} ion in $\text{MgTiO}_3:\text{Fe}^{3+}$ system provides useful information on the single-ion anisotropy to be expected in the antiferromagnetic ilmenite, which is consistent with Haider and Edgar [4]. In general, the doped system is regarded as isotropy in the calculation of the spin-orbit coupling interaction, which has been extensively used in the study of the ground state zero-field splitting. However, it is noted that this method is successful only for molecules, in which the differences between the spin-orbit coupling component parallel to the C_3 axis and the other one perpendicular to the C_3 axis are negligible. Since the layered antiferromagnet MgTiO_3 has obviously trigonal distortion, it is predicted that there might exist discrepancy between the horizontal spin-orbit coupling coefficient and the perpendicular spin-orbit coupling coefficient when Fe^{3+} ion dopes in MgTiO_3 crystal, therefore, we suggest that the anisotropy divergent effect should be considered. According to this point, we quantitatively calculate the EPR second-order and fourth-order parameters D and $(a - F)$ by diagonalizing the complete energy matrices for a d^5 configuration ion in a trigonal ligand-field. The results are consistent with earlier proposal that Fe^{3+} ions can occupy both the Mg^{2+} and Ti^{4+} sites [3–8]. The EPR data for MgTiO_3 containing Fe^{3+} indicate that the anisotropy of Fe^{3+} ion in the diamagnetic ilmenite is not negligible, moreover, the effect

* This project was supported by National Natural Science Foundation of China (No. 10374068).

^a Corresponding author: e-mail: scu_kxy@163.com

of the anisotropy divergent parameter on the second-order parameter D is obviously larger than that on the fourth-order parameter $(a - F)$.

2 Theoretical analyses

The perturbation Hamiltonian for a d^5 configuration ion in a trigonal ligand-field may be expressed as [9]

$$\hat{H} = \hat{H}_{ee} + \hat{H}_{so} + \hat{H}_{CF} = \sum_{i < j} e^2/r_{i,j} + \zeta \sum_i l_i \cdot s_i + \sum_i V_i \quad (1)$$

where \hat{H}_{ee} denotes the electrostatic repulsion energy, \hat{H}_{so} denotes the spin-orbit coupling energy and \hat{H}_{CF} denotes the crystal field potentials. According to the irreducible representations $\Gamma_4(\Gamma_5)$ and Γ_6 of the C_3^* double group, two 84×84 energy matrices corresponding to the perturbation Hamiltonian (1) have been derived [9]. The matrix elements are the function of the Racah parameters B and C , the spin-orbit coupling coefficient ζ and the ligand-field parameters that are in the following forms [10]:

$$\begin{aligned} B_{20} &= \left(\frac{5}{4\pi}\right)^{1/2} \gamma_{20} \langle r^2 \rangle, \\ B_{40} &= 3 \left(\frac{1}{4\pi}\right)^{1/2} \gamma_{40} \langle r^4 \rangle, \\ B_{43}^c &= \frac{3}{2} \left(\frac{1}{2\pi}\right)^{1/2} \gamma_{43}^c \langle r^4 \rangle, \\ B_{43}^s &= i \frac{3}{2} \left(\frac{1}{2\pi}\right)^{1/2} \gamma_{43}^s \langle r^4 \rangle. \end{aligned} \quad (2)$$

For Fe^{3+} in $\text{MgTiO}_3:\text{Fe}^{3+}$ system, the local symmetry may be approximated as C_{3v} . We use p_1, p_2 represent the ligand ions in the up and down pyramids in MO_6 ($M = \text{Mg}$ or Ti) octahedron respectively and θ_1, θ_2 the corresponding angles between metal-ligand bonds and C_3 axis. In this case the explicit expression of B_{kq} may be written as:

$$\begin{aligned} B_{20} &= \frac{3}{2} [G_2(p_1) (3 \cos^2 \theta_1 - 1) + G_2(p_2) (3 \cos^2 \theta_2 - 1)] \\ B_{40} &= \frac{3}{8} [G_4(p_1) (35 \cos^4 \theta_1 - 30 \cos^2 \theta_1 + 3) + G_4(p_2) \\ &\quad \times (35 \cos^4 \theta_2 - 30 \cos^2 \theta_2 + 3)] \\ B_{43}^c &= \frac{3}{4} \sqrt{35} [G_4(p_1) \cos \theta_1 \sin^3 \theta_1 + G_4(p_2) \cos \theta_2 \sin^3 \theta_2] \end{aligned} \quad (3)$$

where $G_2(p_i)$ and $G_4(p_i)$ are expressed as:

$$\begin{aligned} G_2(p_i) &= qeG^2(p_i), \\ G_4(p_i) &= qeG^4(p_i), \end{aligned} \quad (4)$$

$$G^k(p_i) = \int_0^{R_{p_i}} R_{3d}^2(r) r^2 \frac{r^k}{R_{p_i}^{k+1}} dr + \int_{R_{p_i}}^\infty R_{3d}^2(r) r^2 \frac{R_{p_i}^k}{r^{k+1}} dr. \quad (5)$$

Since the bond lengths in the two octahedra in $\text{MgTiO}_3:\text{Fe}^{3+}$ are not the same, we may predict that

$$\begin{aligned} G_2(p_1) &\neq G_2(p_2), \\ G_4(p_1) &\neq G_4(p_2). \end{aligned} \quad (6)$$

According to the Van Vleck approximation for $G^k(p_i)$ integral and using the point charge model [11], we have the following relations:

$$\begin{aligned} G_2(p_2) &= (R_{p_1}/R_{p_2})^3 G_2(p_1), \\ G_4(p_2) &= (R_{p_1}/R_{p_2})^5 G_4(p_1), \end{aligned} \quad (7)$$

where

$$G_4(p_1) = \frac{2G_4}{1 + (R_{p_1}/R_{p_2})^5}, \quad G_2(p_1) = \frac{2G_2}{1 + (R_{p_1}/R_{p_2})^3}.$$

By using the radial wave function of Fe^{3+} ion in complexes [12] and considering the bond lengths in $\text{MgTiO}_3:\text{Fe}^{3+}$, the ratio of G_2 to G_4 for Mg^{2+} site and for Ti^{4+} site are estimated to be 1.54 and 1.37, respectively. With use of the equations (3) and (7), the optical parameters B, C, ζ and D_q of Fe^{3+} in $\text{MgTiO}_3:\text{Fe}^{3+}$ and the energy matrices [9], we can study the relationship between the local lattice structure and the EPR parameters D and $(a - F)$.

The EPR spectrum of a $3d^5$ ion in a trigonal symmetry field can be analyzed in terms of the following spin Hamiltonian given by Bleaney and Trenam [13]:

$$\begin{aligned} \hat{H}_S &= g\beta \hat{H} \cdot \hat{S} + D [S_z^2 - (1/3)S(S+1)] \\ &\quad + (1/6)a [S_\xi^4 + S_\eta^4 + S_\zeta^4 - (1/5)S \\ &\quad \times (S+1)(3S^2 + 3S - 1)] \\ &\quad + (1/180)F [35S_z^4 - 30S(S+1)S_z^2 \\ &\quad + 25S_z^2 - 6S(S+1) + 3S^2(2S+1)^2] \end{aligned} \quad (8)$$

where D and F correspond to axial component of the second-order and the fourth-order respectively. a is the cubic field splitting parameter. The energy eigenvalues of ground state 6A_1 for a zero magnetic field are given as follows:

$$\begin{aligned} E(\pm 1/2) &= (1/3)D - (1/2)(a - F) \\ &\quad - (1/6) [(18D + a - F)^2 + 80a^2]^{1/2}, \\ E(\pm 3/2) &= -(2/3)D + (a - F), \\ E(\pm 5/2) &= (1/3)D - (1/2)(a - F) \\ &\quad + (1/6) [(18D + a - F)^2 + 80a^2]^{1/2}. \end{aligned} \quad (9)$$

Then the 6A_1 ground state zero-field splitting energy ΔE_1 and ΔE_2 can be expressed as [14]:

$$\begin{aligned} \Delta E_1 &= (\pm 1/3) [(18D + a - F)^2 + 80a^2]^{1/2}, \\ \Delta E_2 &= (3/2)(a - F) - D \pm (1/6) \\ &\quad \times [(18D + a - F)^2 + 80a^2]^{1/2}, \end{aligned} \quad (10)$$

where the signs “+” and “-” correspond to $D \geq 0$ and $D < 0$ respectively. Kuang had shown that the low-symmetry EPR parameters D and $(a - F)$ are almost independent of the EPR cubic parameter a for Fe^{3+} in Al_2O_3 [9], and Yu had given the expressions of the EPR parameters D , F and a by using high order perturbation method [15]:

$$\begin{aligned} D &= (1/28)[5W(5/2, 5/2) - W(3/2, 3/2) \\ &\quad - 4W(1/2, 1/2)], \\ F &= \left(-3/2\sqrt{5}\right)W(5/2, -1/2) + (3/14)[W(5/2, 5/2) \\ &\quad + 2W(1/2, 1/2) - 3W(3/2, 3/2)], \\ a &= \left(-3/2\sqrt{5}\right)W(5/2, -1/2), \end{aligned} \quad (11)$$

where $W(M_S, M'_S)$ denotes perturbation matrix elements. From equation (11), We can see that the $(a - F)$ parameter is not related to cubic parameter a . Therefore, the low-symmetry EPR parameters D and $(a - F)$ can be determined by employing cubic parameter a , ΔE_1 and ΔE_2 which can be obtained by diagonalizing complete energy matrices.

3 Isotropy calculations

In the local crystalline structure of MgTiO_3 , which has the similarly trigonal crystal structure of Al_2O_3 , the cations Mg^{2+} and Ti^{4+} both occupy octahedral sites with C_3 symmetry. When $3d^5$ ions dope in MgTiO_3 , McClure suggested that the $3d^5$ ion does not occupy the exact site of the replaced host ion, but is displaced along the C_3 axis by an amount ΔZ because the repulsive force acting on the impurity differs from that on the host ion [15]. By taking z -axis along C_3 axis of MgTiO_3 , the local distortion may be described by using a displacement ΔZ as plotted in Figure 1. $\Delta Z > 0$ and $\Delta Z < 0$ represent the shift of impurity ion towards up and down oxygen triangles, respectively. If one use R_{10} , R_{20} , θ_{10} and θ_{20} to represent the Mg(Ti)-O bond lengths and the angles between Mg(Ti)-O bond and C_3 axis in the up and down pyramids in host crystal MgTiO_3 , respectively, then the local structure parameters R_1 , R_2 , θ_1 and θ_2 for impurity ions replacing the host ions in MgTiO_3 system can be expressed as:

$$\begin{aligned} R_1 &= \left[(R_{10} \sin \theta_{10})^2 + (R_{10} \cos \theta_{10} - \Delta Z)^2 \right]^{1/2}, \\ R_2 &= \left[(R_{20} \sin \theta_{20})^2 + (R_{20} \cos \theta_{20} + \Delta Z)^2 \right]^{1/2}, \\ \theta_1 &= \text{tg}^{-1} \left(\frac{L_{10}}{R_{10} \cos \theta_{10} - \Delta Z} \right), \\ \theta_2 &= \text{tg}^{-1} \left(\frac{L_{20}}{R_{20} \cos \theta_{20} + \Delta Z} \right), \end{aligned} \quad (12)$$

where L_{10} and L_{20} are the distances between O^{2-} and threefold axis in the up and down oxygen triangles, respectively [16]. Thereby, the relationship between the distortion of local lattice structure of Fe^{3+} in $\text{MgTiO}_3:\text{Fe}^{3+}$ system and the EPR parameters D , $(a - F)$ can be studied

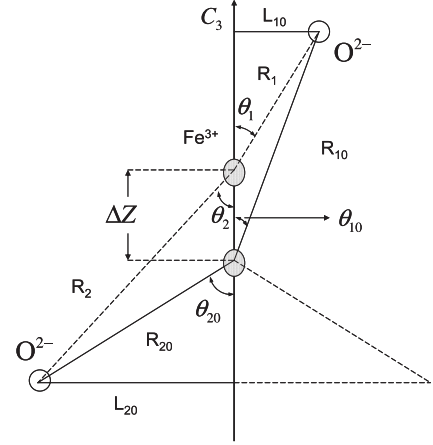


Fig. 1. Displacement model of Fe^{3+} in MgTiO_3 $R_{10} = 2.19$ Å, $R_{20} = 2.04$ Å, $\theta_{10} = 45.2^\circ$, $\theta_{20} = 63.8^\circ$; $R_{10} = 2.12$ Å, $R_{20} = 1.89$ Å, $\theta_{10} = 47.0^\circ$, $\theta_{20} = 64.7^\circ$ [6] for Mg^{2+} and Ti^{4+} sites, respectively. R_1 , R_2 , θ_1 , θ_2 are the structure parameters when Fe^{3+} replaces Mg^{2+} or Ti^{4+} site, ΔZ represents the shift along the threefold axis.

by diagonalizing the complete energy matrices and with use of the optical parameters B and C , the spin-orbit coupling coefficient ζ and the cubic ligand-field parameter Dq . For Fe^{3+} in $\text{MgTiO}_3:\text{Fe}^{3+}$ system, to our knowledge, no optical spectra data were reported. However, one can estimate its spectral parameters from the spectral parameters of $\text{Al}_2\text{O}_3:\text{Fe}^{3+}$ system because of the similarly local structure of MgTiO_3 and Al_2O_3 crystals. Thus, we have $B = 660$ cm^{-1} , $C = 3135$ cm^{-1} , $\zeta = 360$ cm^{-1} [17–19], and $G_4 = 8790$ cm^{-1} for Mg^{2+} site and $G_4 = 8940$ cm^{-1} for Ti^{4+} site, respectively, where $G_4 = 6|D_q|$ and D_q is the ligand-field strength. By taking the optical parameters of Fe^{3+} in $\text{MgTiO}_3:\text{Fe}^{3+}$ system, we calculate the EPR second-order and fourth-order parameters D and $(a - F)$ vs. the displacement ΔZ by diagonalizing the energy matrices of the electron-electron repulsion, the ligand-field and the spin-orbit coupling interaction for a d^5 configuration ion in a trigonal ligand-field. The calculated results are listed in Table 1. It is remarkable that, if the system is regarded as isotropy, the calculated EPR second-order and fourth-order parameters D and $(a - F)$ of Fe^{3+} in MgTiO_3 cannot agree well with experimental data, simultaneously, i.e. although the calculated EPR second-order parameter $10^4 D_{\text{calc.}} = 845.5$ cm^{-1} for $\Delta Z = 0.0888$ Å in Mg^{2+} site; $10^4 D_{\text{calc.}} = 784.9$ cm^{-1} for $\Delta Z = 0.1711$ Å in Ti^{4+} site can agree well with the experimental findings [4], however, we also note that the calculated EPR fourth-order parameter $(a - F)$ deviates far from the experimental data and this obvious difference cannot be removed by employing the other group of the optical parameters in the calculations. This implies that regarding the $\text{MgTiO}_3:\text{Fe}^{3+}$ system as isotropy may not be adequate in accounting for the ground state zero-field splitting. In order to simultaneously explain the EPR second-order and fourth-order parameters D and $(a - F)$ for Fe^{3+} in $\text{MgTiO}_3:\text{Fe}^{3+}$ system, the anisotropy

Table 1. The ground state zero-field splitting ΔE_1 , ΔE_2 and the EPR parameters a , D and $(a - F)$ for the octahedral Fe^{3+} centers in MgTiO_3 , regarding the system as isotropy.

	ΔZ (Å)	ζ (cm^{-1})	$10^4 \Delta E_1$ (cm^{-1})	$10^4 \Delta E_2$ (cm^{-1})	$10^4 D$ (cm^{-1})	$10^4(a - F)$ (cm^{-1})	$10^4 a$ (cm^{-1})
Mg^{2+} Site	0	360	9467.4	3315.9	1571.8	102.6	75.7
	0.02		8521.1	3006.8	1413.8	106.7	75.7
	0.04		7545.2	2688.1	1250.8	110.9	75.7
	0.06		6553.2	2364.1	1085.2	115.1	75.7
	0.0888		5118.6	1895.6	845.5	121.2	75.7
	0.10		4566.5	1715.6	753.3	123.8	75.7
	Ref. [4]		5114.0	1884.7	845.1	115.2	75.7
	Ti^{4+} site	0	360	13132.6	4561.3	2181.9	117.9
0.04			11268.4	3955.2	1870.6	127.7	78.3
0.076			9454.2	3364.1	1567.6	136.4	78.3
0.12			7201.4	2630.6	1191.4	147.5	78.3
0.1711			4768.2	1839.5	784.9	160.2	78.3
0.18			4384.0	1714.8	720.6	162.3	78.3
Ref. [4]			4769.1	1803.5	786.3	136.8	78.3

spin-orbit coupling mechanism will be considered in the following calculation.

4 Anisotropy spin-orbit coupling interaction

Since the local structure of MgTiO_3 has obviously trigonal distortion, it is reasonable to predict that when the transition-metal ion Fe^{3+} dopes in MgTiO_3 system, the distorted ligand-field will give rise to an anisotropy effect on the spin-orbit coupling interaction and causes the difference between the horizontal spin-orbit coupling coefficient and the perpendicular spin-orbit coupling coefficient. Considering the anisotropy, in general, the operator of the spin-orbit coupling can be expressed as:

$$\hat{H}_{so} = \zeta_{\parallel} \hat{L}_z \hat{S}_z + \zeta_{\perp} (\hat{L}_+ \hat{S}_- + \hat{L}_- \hat{S}_+)/2, \quad (13)$$

in which ζ_{\parallel} , ζ_{\perp} are the horizontal and perpendicular spin-orbit coupling coefficients, respectively. For the clarity in physics, we introduce two parameters ζ_1 and ζ_2 as follows [20]:

$$\begin{aligned} \zeta_1 &= (\zeta_{\parallel} + 2\zeta_{\perp})/3, & \zeta_2 &= (\zeta_{\parallel} - \zeta_{\perp})/2, \\ \zeta_{\parallel} &= \zeta_1 + (4/3)\zeta_2, & \zeta_{\perp} &= \zeta_1 - (2/3)\zeta_2. \end{aligned} \quad (14)$$

The physical meanings of ζ_1 and ζ_2 are the average and the divergent values of the horizontal and perpendicular components of spin-orbit coupling coefficient, respectively. Starting from the equation (13) we can obtain the anisotropy spin-orbit coupling matrices for a d^5 configuration ion in a trigonal ligand-field. The direct anisotropy spin-orbit coupling matrix elements between the ${}^6\text{S}$ and the ${}^4\text{P}$ states are listed in Table 2. From Table 2, we can

Table 2. The direct anisotropy spin-orbit coupling matrix elements between the ${}^6\text{S}$ and the ${}^4\text{P}$ states.

$\text{H}_{s.o}$	$ {}^4P, \frac{1}{2}, \pm\frac{1}{2}\rangle$	$ {}^4P, \frac{3}{2}, \pm\frac{1}{2}\rangle$	$ {}^4P, \frac{5}{2}, \pm\frac{1}{2}\rangle$
$\langle {}^6S, \frac{5}{2}, \pm\frac{1}{2} $	$(\zeta_{\parallel} - \zeta_{\perp})$	$\mp \frac{\sqrt{5}}{5} (\zeta_{\parallel} - \zeta_{\perp})$	$-\frac{\sqrt{5}}{5} (3\zeta_{\parallel} + 2\zeta_{\perp})$
$\text{H}_{s.o}$		$ {}^4P, \frac{3}{2}, \pm\frac{3}{2}\rangle$	$ {}^4P, \frac{5}{2}, \pm\frac{3}{2}\rangle$
$\langle {}^6S, \frac{5}{2}, \pm\frac{3}{2} $		$\mp \frac{\sqrt{30}}{5} (\zeta_{\parallel} - \zeta_{\perp})$	$-\frac{\sqrt{5}}{5} (2\zeta_{\parallel} + 3\zeta_{\perp})$
$\text{H}_{s.o}$			$ {}^4P, \frac{5}{2}, \pm\frac{5}{2}\rangle$
$\langle {}^6S, \frac{5}{2}, \pm\frac{5}{2} $			$-\sqrt{5}\zeta_{\perp}$

see that in the condition of $\zeta_{\parallel} = \zeta_{\perp}$, the anisotropy spin-orbit coupling matrices can degenerate into the case of the isotropy. One of the most interesting things is to study the contribution of the anisotropy divergent parameter ζ_2 to the ground state zero-field splitting. In present work, we have derived the Kramers levels of the ${}^6\text{A}_1$ state as a function of the divergent spin-orbit coupling parameter ζ_2 by diagonalizing the complete energy matrices. It is worthwhile to point out that the ground state zero-field splitting of Fe^{3+} ion in MgTiO_3 depends sensitively on the anisotropy divergent parameter ζ_2 (see Tab. 3). Table 3 clearly shows that the value of the ${}^6\text{A}_1$ ground state splittings goes high as the ζ_2 value increases and the change of second-order parameter D is more distinct than that of the fourth-order parameter $(a - F)$. In order to accurately determine the ground state zero-field splitting of Fe^{3+} in $\text{MgTiO}_3:\text{Fe}^{3+}$ system, again the energy matrices as well as the optical parameters are employed. The calculations of the EPR second-order and fourth-order parameters D and $(a - F)$ vs. the divergent spin-orbit coupling parameter ζ_2 and the displacement ΔZ are accomplished by diagonalizing the energy matrices. As shown in Table 4, both the calculated EPR

Table 3. The relationship between Kramers levels in 6A_1 state and the anisotropy divergent parameter ζ_2 for Fe^{3+} in $\text{MgTiO}_3:\text{Fe}^{3+}$ system, units are in cm^{-1} .

Mg ²⁺ site						Ti ⁴⁺ site					
ζ_1	ζ_2	$\Delta E_1 \times 10^4$	$\Delta E_2 \times 10^4$	D	$a - F$	ζ_1	ζ_2	$\Delta E_1 \times 10^4$	$\Delta E_2 \times 10^4$	D	$a - F$
360	-1.0	7312.9	2596.6	1212.6	101.8	360	-2.0	8731.4	3092.4	1448.2	116.6
	-0.8	7743.6	2740.6	1284.4	102.1		-1.92	8907.6	3151.0	1477.6	116.6
	-0.6	8174.4	2884.4	1356.2	102.3		-1.5	9830.0	3458.9	1631.4	116.8
	-0.4	8605.1	3028.0	1428.0	102.3		-1.0	10929.7	3825.8	1814.7	117.1
	-0.2	9035.9	3171.6	1499.8	102.3		-0.5	12030.9	4193.2	1998.3	117.3
	0	9467.4	3315.9	1571.8	102.6		0	13132.6	4561.3	2181.9	118.0
	0.2	9899.3	3459.8	1643.8	102.6		0.5	14236.1	4929.6	2365.8	118.2
	0.4	10330.5	3603.8	1715.6	102.8		1.0	15340.3	5298.4	2549.8	118.7
	0.6	10762.0	3747.6	1787.6	102.8		1.5	16445.4	5667.2	2734.0	119.0
	0.8	11194.4	3892.2	1859.6	103.1		1.92	17374.6	5977.2	2888.9	119.2
	1.0	11626.2	4035.8	1931.6	102.9		2.0	17551.8	6036.5	2918.4	119.4
Expt. [4]		5114.0	1884.7	845.1	115.2	Expt. [4]		4769.1	1803.5	786.3	136.8

Table 4. The ground state zero-field splitting ΔE_1 , ΔE_2 and the EPR parameters a , D and $(a - F)$ for the octahedral Fe^{3+} centers in MgTiO_3 considering the anisotropy effect.

	ΔZ	ζ_1	ζ_2	$10^4 \Delta E_1$	$10^4 \Delta E_2$	$10^4 D$	$10^4 (a - F)$	$10^4 a$
	(Å)	(cm^{-1})	(cm^{-1})	(cm^{-1})	(cm^{-1})	(cm^{-1})	(cm^{-1})	(cm^{-1})
Mg ²⁺ site	0	360	-0.6	8174.4	2884.4	1356.2	102.3	75.7
	0.02			7220.1	2572.8	1196.9	106.4	75.7
	0.04			6237.2	2251.3	1032.7	110.3	75.7
	0.06			5238.5	1925.2	865.9	114.6	75.7
	0.0625			5113.1	1884.3	845.0	115.1	75.7
	0.08			4234.6	1597.5	698.2	118.9	75.7
	0.10			3239.6	1273.2	531.8	123.4	75.7
	Ref. [4]			5114.0	1884.7	845.1	115.2	75.7
Ti ⁴⁺ site	0	360	-1.92	8907.6	3151.0	1477.6	116.6	78.3
	0.02			7973.1	2847.2	1321.5	121.5	78.3
	0.04			6986.1	2525.9	1156.7	126.3	78.3
	0.06			5960.2	2191.8	985.3	131.3	78.3
	0.08			4913.0	1850.2	810.3	136.0	78.3
	0.0827			4770.8	1804.2	786.6	136.9	78.3
	0.10			3861.0	1507.7	634.5	141.1	78.3
	Ref. [4]			4769.1	1803.5	786.3	136.8	78.3

second-order and fourth-order parameters D and $(a - F)$ of Fe^{3+} in $\text{MgTiO}_3:\text{Fe}^{3+}$ system agree well with the experimental findings with $\zeta_2 = -0.6 \text{ cm}^{-1}$, $\Delta Z = 0.0625 \text{ Å}$ for Mg^{2+} site; $\zeta_2 = -1.92 \text{ cm}^{-1}$, $\Delta Z = 0.0827 \text{ Å}$ for Ti^{4+} site, respectively. Our results imply that the anisotropy spin-orbit coupling effect is important and the anisotropy is not negligible in studying the Fe^{3+} ion in the diamagnetic ilmenite $\text{MgTiO}_3:\text{Fe}^{3+}$ system. This opinion is consistent with Haider and Edgar [4]. From our calculation, we have determined that the Fe^{3+} ions can occupy both the Mg^{2+} and Ti^{4+} sites, which may explain why the EPR spectrum of iron doping, unlike manganese doping, is not

very intense [3]. The results are consistent with the earlier findings reported by experiments [3–5].

5 Conclusions

The anisotropy spin-orbit coupling matrices for a d^5 configuration ion in a trigonal ligand-field have been established. The ground state zero-field splitting of Fe^{3+} ion in $\text{MgTiO}_3:\text{Fe}^{3+}$ system has been investigated by considering the anisotropy spin-orbit coupling interaction. It is noted that the EPR parameters, especially the

low-symmetry second-order parameter D , depend sensitively on the anisotropy divergent parameter ζ_2 . The results demonstrate that the experimental EPR parameters D and $(a - F)$ of Fe^{3+} in $\text{MgTiO}_3:\text{Fe}^{3+}$ system can be satisfactorily explained by considering the contributions of the anisotropy divergent parameter ζ_2 to the ground state zero-field splitting. It is confirmed that the Fe^{3+} ions can occupy both the Mg^{2+} and Ti^{4+} sites for $\zeta_2 = -0.6 \text{ cm}^{-1}$, $\Delta Z = 0.0625 \text{ \AA}$ and $\zeta_2 = -1.92 \text{ cm}^{-1}$, $\Delta Z = 0.0827 \text{ \AA}$ respectively, which are consistent with the experimental findings.

This project was supported by National Natural Science Foundation of China (No. 10374068) and the Doctoral Education Fund of Education Ministry of China (No.20050610011).

References

1. S.Y. Wu, X.Y. Guo, W.Z. Yan, *J. Mole. Struc.* **668**, 249 (2004)
2. D. Padro, A.P. Howes, M.E. Smith, R. Dupree, *Solid State Nuclear Resonance* **15**, 231 (2000)
3. E. Lopez Carranza, R.T. Cox, *J. Phys. Chem. Solids* **40**, 413 (1979)
4. A.F.M.Y. Haider, A. Edgar, *J. Phys. C: Solid St. Phys.* **13**, 6239 (1980)
5. J. Vega Lino, E. Lopez Carranza, A. Valera Palacios, *Solid State Communications* **33**, 729 (1980)
6. W.C. Zheng, *Radiation Effects and Defects in Solids* **127**, 231 (1993)
7. W.C. Zheng, *J. Phys. Chem. Solids* **56**, 61 (1995)
8. W.C. Zheng, *J. Phys. Chem. Solids* **55**, 647 (1994)
9. X.Y. Kuang, *Phys. Rev. B* **36**, 712 (1987); X.Y. Kuang, *Phys. Rev. B* **36**, 797 (1987)
10. D.J. Newman, W. Urban, *Adv. Phys.* **24**, 793 (1975)
11. J.H. Van. Vleck, *J. Chem. Phys.* **1**, 208 (1932)
12. X.Y. Kuang, Q.Q. Gou, K.W. Zhou, *Phys. Lett. A* **293**, 293 (2002)
13. B. Bleaney, R.S. Trenam, *Proc. R. Soc. London, Ser. A* **233**, 1 (1954)
14. A. Abragam, B. Bleaney, *Electron Paramagnetic Resonance of Transition Ions* (Oxford University Press, Oxford, 1986)
15. W.L. Yu, *Chinese Science Bulletin* **38**, 1283 (1993)
16. D.S. McClure, *J. Chem. Phys.* **38**, 2289 (1963)
17. T.H. Yeom, Y.M. Chang, S.H. Choh, *Phys. Stat. Sol (b)* **185**, 409 (1994)
18. L. Li, T.R. Zhang, W.L. Yu, *J. SiChuan, Normal University (Natural Science)* **21**, 288 (1998)
19. W.C. Zheng, *Physica B* **245**, 119 (1998)
20. X.Y. Kuang, Irene Morgenstern-Badarau, *J. Phys. Soc. Jpn* **63**, 3901 (1994)